Optimal design and test of the flexible clamping device for safflower

Shuangping Yang[1,2*], Zhenguo Zhang[1], Gang Guo[1], Yi Zhang[1], Shilong Qiu[1], Yunxia Ye[1]
(1. *College of Mechanical and Electrical Engineering, Xinjiang Agricultural University, Urumqi 830052, China*;
2. *Key Laboratory of Xinjiang Intelligent Agricultural Equipment, Urumqi 830052, China*)

Abstract: Aiming to address the issues of inconvenience and low efficiency associated with manual harvesting of safflower silk and the high damage rate of cutting harvesting machinery, the effect of manual grasping and drawing was simulated and a safflower drawing and harvesting device was designed based on flexible clamping. A quadratic regression orthogonal rotation combination design was implemented, adopting clamping frequency, spring installation angle, and flower board angle as factors while targeting removal and damage rates as performance metrics. Analysis identified clamping frequency as the predominant factor governing device recovery rate, with spring installation angle and flower board angle exerting secondary influence. Spring installation angle emerged as the dominant factor affecting device damage rate, followed sequentially by flower board angle and clamping frequency. The optimal parameters of the harvesting device are as follows: clamping frequency of 50 times/min, initial installation angle of the spring of 3.2°, and an initial angle of the flower board of 25°. Field tests with optimized parameters demonstrated a 96.28% removal rate and a 2.29% damage rate. The research findings can provide theoretical guidance for the structural design and optimization of the mechanized harvesting device for safflower filaments.
Keywords: agricultural engineering, safflower, harvest, clamping, test
DOI: 10.25165/j.ijabe.20251803.8536

Citation: Yang S P, Zhang Z G, Guo G, Zhang Y, Qiu S L, Ye Y X. Optimal design and test of the flexible clamping device for safflower. Int J Agric & Biol Eng, 2025; 18(3): 19–24.

1 Introduction

Safflower is an important cash crop whose filaments have been used as food coloring agents and possess high medicinal value[1-4]. Xinjiang, China is the largest producer of safflower, accounting for over 80% of the national total[5,6]. As safflower filaments can be harvested from the flower bulbs two to three times, it is necessary to avoid damaging the flower buds and stems during the harvesting process[7]. Additionally, the flowering period of safflower is short, and the filaments are only suitable for harvesting within 1-5 d after flowering[8], resulting in labor-intensive manual harvesting with low efficiency. Therefore, there is an urgent need to develop mechanized safflower harvesting devices to reduce labor intensity and improve harvesting efficiency.

For the harvesting of safflower filaments, the existing harvesting machinery is mainly a manual auxiliary harvesting equipment[9,10]. Specifically, it can be divided into two types: cutting type and pulling type. Cutting type refers to the harvesting of filigree by cutting the filament with a knife head[11,12]. A typical example is the progressive rotary cutting safflower harvesting device developed by Zhang et al.[13,14], which uses a rotating progressive tool to cut the filament. The device utilizes sensors to detect whether the filigree is fully within the cutting range, which reduces the filament damage rate compared to ordinary cutting methods.

Pulling type refers to the harvesting of filaments by pulling them off the flower bud[15-17]. A typical example is the roller-type filament pulling and harvesting device developed by Ge et al.[7,8,18] This device utilizes two high-speed rotating rubber rollers to pull and harvest the filament, resulting in a relatively low filament breakage rate. However, due to the corrosion and hardening of the rubber rollers, the rigid contact of the filament leads to an increased filament breakage rate. In summary, as pulling type harvests the filament out of the flower bud, the remaining filament content in the bud after harvesting is lower, meaning more filament is harvested. Cutting type is primarily a way to cut off filaments, which achieves lower harvest benefits. Therefore, pulling type is the primary method for harvesting safflower.

Based on the above, a flexible safflower clamping device was designed that utilizes spring elasticity to avoid the rigid contact of the filament and reduce damage caused during the drawing process, thereby improving the quality of filament harvesting and increasing the efficiency of filament collection while reducing labor intensity. Additionally, through test analysis, the optimal combination of working parameters has been determined and verified, providing technical guidance for the subsequent design of safflower harvesting machines.

2 Structure and principle

2.1 Overall structure

The safflower flexible clamping device is shown in Figure 1, which consists of a shield, a clamping mechanism, a motor, and a negative pressure suction port. The clamping mechanism is mounted inside the shield, which consists of three clipping arms, three springs, an eccentric disc, and a piston push rod. The power of the clamping mechanism is provided by the motor. The negative pressure suction port is mounted on the upper part of the shield and is used to collect the filigree that is removed from the clip.

Received date: 2023-09-20 **Accepted date:** 2025-05-15
Biographies: Zhenguo Zhang, PhD, Associate Professor, research interest: precision agriculture, Email: bigbearsun@163.com; **Gang Guo**, MS, Lecturer, research interest: facility agriculture, Email: 2692191092@qq.com; **Yi Zhang**, MS, Lecturer, research interest: application of sensors in agriculture, Email: 774195006@qq.com; **Shilong Qiu**, MS, Lecturer, research interest: conservation tillage and equipment, Email: 527361636@qq.com; **Yunxia Ye**, MS, Associate Professor, research interest: residual film recovery equipment, Email: 2496061824@qq.com.
***Corresponding author: Shuangping Yang**, MS, Lecturer, research interest: agricultural mechanized harvesting device. College of Mechanical and Electrical Engineering, Xinjiang Agricultural University, Urumqi 830052, China. Tel: +86-18299125990, Email: ysp845@126.com.

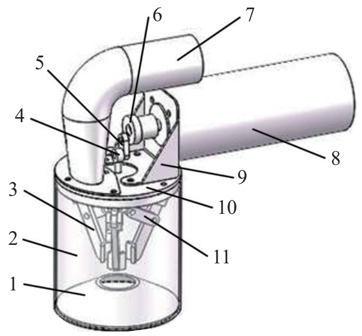

1. Shirk 2. Shield 3. Clipping arm 4. Piston push rod 5. Pulled connecting rod 6. Eccentric disc 7. Negative pressure suction port 8. Motor 9. Motor retention 10. Cover plate 11. Pulling rod

Figure 1 Safflower flexible clamping device

2.2 Working principle

The safflower flexible clamping mechanism workflow is shown in Figure 2. Figure 2a illustrates the initial preparation phase, where the spring is in its relaxed state and the piston pusher is at its lowest position. At this point, the clip plate is in an open configuration. As the piston push rod is driven upwards by the motor, the upper part of the clip arm is relatively fixed due to the spring preload, while the lower end of the clip arm is tightened until the midline position, clamping the filament, as shown in Figure 2b. As the piston push rod continues to move upwards, the spring is compressed, and the flower board at the lower end of the clip arm clamps onto the filament and moves upwards, confining the flower ball to the bottom of the housing, thereby pulling the filament off the flower ball. During this process, the spring's elastic clamping force avoids rigid contact with the filament, reducing damage to it during harvesting.

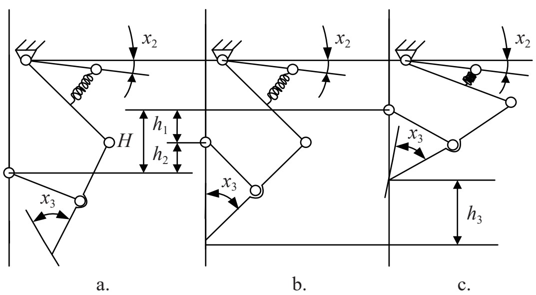

Note: x_2 is the initial installation angle of spring, (°); x_3 is the initial angle of the flower board, (°); h_1 is the height that the piston rises during filigree pulling, mm; h_2 is the height that the piston rises during filigree clamping, mm; h_3 is the height of the filigree movement, mm; H is the total stroke of the piston, mm.

Figure 2 Working principle

During the return of the piston push rod, the spring continues to compress and the clip arm tapes the flower to the position shown in Figure 2b. As the piston push rod is continuously moved downwards, the clip arm opens up, as shown in Figure 2a. At this point, the filaments removed from the clip are subject to the influence of negative pressure and are carried along the piping into the collection box, completing the harvesting process.

3 Materials and methods

3.1 Experimental materials

Yumin thornless safflower was selected as the experimental material, which was planted in Yumin county of Xinjiang Autonomous Region. The average length of the flower petals is 10.4 mm, the average diameter of the safflower cone is 21.4 mm, and the moisture content of the flower petals is between 70% and 80%[8,19,20].

3.2 Experimental device

The experimental device consists of a negative pressure fan, a motor, and a clamping mechanism, as shown in Figure 3.

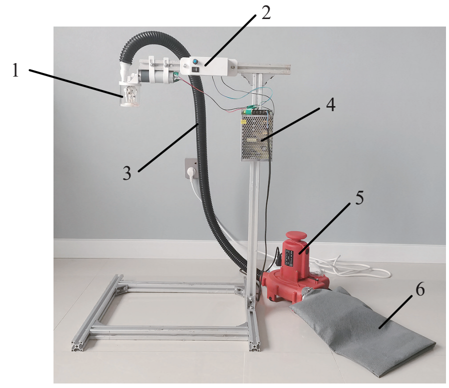

1. Safflower flexible clamping device 2. Controller 3. Pipeline 4. Transformer 5. Negative pressure fan 6. Flower collecting bag

Figure 3 Clamping experimental device

The negative pressure in the suction port and shield is provided by the negative pressure fan, and it can be fixed to a constant value. The power of the eccentric disc is provided by the motor, and the rotation speeds of the motor were controlled by frequency converter. The initial installation angle of the spring can be adjusted by tightening the set screw, thereby changing the size of the clamping force. The angle of the clip plate and the clip arm, which is the initial angle of the flower board, can be adjusted by changing the clipping arm. The shield was transparent in order to observe the movement of the clamping mechanism and the state of the safflower filaments. The parameters of the experimental device are listed in Table 1.

Table 1 Parameters of the experimental device

Parameter	Value
Size of clamping device (length×width×height)/mm	150×60×110
Harvest frequency/r·min^{-1}	0-150
Height of filigree pulling/mm	20
Height of piston motion/mm	10
Angle of swing arm movement/(°)	35-50
Power of negative pressure fan/kW	25

3.3 Experimental index

Safflower was used as the experimental object to study the removal capacity and harvest quality of the harvesting device. According to the pre-experiment, when the initial installation angle of the spring was at a high value, the stronger the clamping force is, the better the removal capacity of the experimental device is. Therefore, the proportion of the mass of the filigree harvested by the device to the total mass at a harvested safflower is an index to investigate the removal capacity. With the improvement of the removal capacity, more clamping force will apply to the filigree, which will cause serious filigree damage. Therefore the proportion of the mass of the damaged filigree to the total mass at collection box is an index of harvest quality.

The calculation of the removal rate is shown in Equation (1)[21,22]:

$$y_1 = \frac{m_1}{m_1 + m_2} \times 100\% \tag{1}$$

where, y_1 is the removal rate; m_1 is the mass of the filigree harvested by the device, g; m_2 is the mass of the filigree remains on the flower bulbs after harvesting, g.

The calculation of the damage rate is shown in Equation (2):

$$y_2 = \frac{m_3}{m_1} \times 100\% \tag{2}$$

where, m_3 is the mass of the filigree obviously damaged in the harvested filigree, g.

3.4 Experimental methods

This experiment is based on the study of anti-flower filigree damaging performance of flexible clamping device. In this experiment, the wind speed at the negative pressure suction port was fixed at 3 m/s. The clamping frequency (x_1), initial installation angle of the spring (x_2), and initial angle of the flower board (x_3) were selected as the experimental factors. The removal rate (y_1) and the damage rate (y_2) were used as the experimental indices.

On the basis of ensuring better harvesting performance of the clamping mechanism, by combining the single factor test of the clamp device, the parameter range of the clamping mechanism was determined: the range of the clamping frequency is 50-70 times/min, the range of the initial installation angle of the spring is 0°-10°, and the range of the initial angle of the flower board is 20°-30°. In order to determine the optimal combination of parameters, Central Composite Design (CCD)[23-27] test schemes were used. The test factors and levels are listed in Table 2, and the test programs and results are listed in Table 3.

Table 2 Coding of experimental factor levels

Level	Factor		
	x_1/(times/min)	x_2/(°)	x_3/(°)
+1	70	10	30
0	60	5	25
–1	50	0	20

Note: x_1 is the clamping frequency; x_2 is the initial installation angle of the spring; x_3 is the range of the initial angle of the flower board.

Table 3 Regression orthogonal experimental results

Number	Factor			Index	
	x_1/(times/min)	x_2/(°)	x_3/(°)	y_1/%	y_2/%
1	50	0	20	93.42	2.16
2	70	0	20	92.07	2.24
3	50	10	20	94.72	2.73
4	70	10	20	92.45	2.62
5	50	0	30	94.56	2.33
6	70	0	30	92.52	2.96
7	50	10	30	95.31	2.62
8	70	10	30	92.73	2.91
9	43.18	5	25	96.25	2.34
10	76.82	5	25	92.96	2.61
11	60	–3.41	25	92.78	2.42
12	60	13.41	25	93.95	2.97
13	60	5	16.59	92.45	2.16
14	60	5	33.41	93.54	2.72
15	60	5	25	96.17	2.43
16	60	5	25	96.28	2.51
17	60	5	25	96.14	2.42
18	60	5	25	95.92	2.34
19	60	5	25	96.17	2.45
20	60	5	25	96.12	2.48

Note: y_1 is the removal rate; y_2 is the damage rate.

4 Results and analysis

4.1 Variance analysis experimental results

The Central Composite Design experiment results are listed in Table 3.

Through regression response analysis by Design-Expert 11, a regression model of the removal rate y_1 and the damage rate y_2 was obtained:

$$y_1 = 96.13 - 1.01X_1 + 0.34X_2 + 0.31X_3 - 0.18X_1X_2 - 0.12X_1X_3 - 0.09X_2X_3 - 0.55X_1^2 - 0.99X_2^2 - 1.12X_3^2 \tag{3}$$

$$y_2 = 2.44 + 0.098X_1 + 0.15X_2 + 0.15X_3 - 0.066X_1X_2 + 0.12X_1X_3 - 0.089X_2X_3 + 0.097X_2^2 \tag{4}$$

Analysis of variance was carried out on the regression model of the removal rate and the damage rate. Variance analysis results are listed in Table 4.

Table 4 Analysis of variance of multi-factor experiment

Source	Removal rate		Damage rate	
	F	p	F	p
Model	524.40	<0.0001**	40.92	<0.0001**
X_1	1359.55	<0.0001**	44.14	<0.0001**
X_2	152.16	<0.0001**	109.30	<0.0001**
X_3	132.09	<0.0001**	98.90	<0.0001**
X_1X_2	26.08	0.0005**	11.72	0.0065**
X_1X_3	12.23	0.0057**	37.65	0.0001**
X_2X_3	6.34	0.0305*	21.03	0.0010*
X_1^2	422.25	<0.0001**	1.74	0.2170
X_2^2	1370.04	<0.0001**	45.05	<0.0001**
X_3^2	1757.88	<0.0001**	0.2113	0.6556
Lack of fit	0.4609	0.7923	0.7541	0.6178

Note: **very significant (p<0.01); *significant (p<0.05); otherwise: not significant (p>0.17).

The factors have significant effects on the two evaluation indices. The misfit value p is less than 0.01, showing a good fitting effect. Removal rate was primarily governed by clamping frequency, followed by spring installation angle and flower board angle. Conversely, spring installation angle dominated damage rate influence, with flower board angle and clamping frequency exerting secondary effects.

4.2 Response surface analysis

Figure 4 shows the influence of the factors on the filigree removal capacity. Figure 5 shows the influence of the factors on the harvest quality. The response surface analysis of the experiment was carried out by Design -Expert 11.

4.2.1 Analysis of effects of the factors on the removal rate

Figure 4a is a response surface diagram of the effect of the clamping frequency and the initial installation angle of the spring on the removal rate when the initial angle of the flower board was 25°. When the clamping frequency was fixed, the removal rate of the safflower filaments first increased and then decreased with the increase of the initial installation angle of the spring. When the initial installation angle of the spring was fixed, the removal rate first increased and then tended to flatten with the decrease of the clamping frequency. The removal rate was the largest when the clamping frequency was 50 times/min and the initial installation angle of the spring was 5°.

Figure 4b is a response surface diagram of the effect of the clamping frequency and the initial angle of the flower board on the

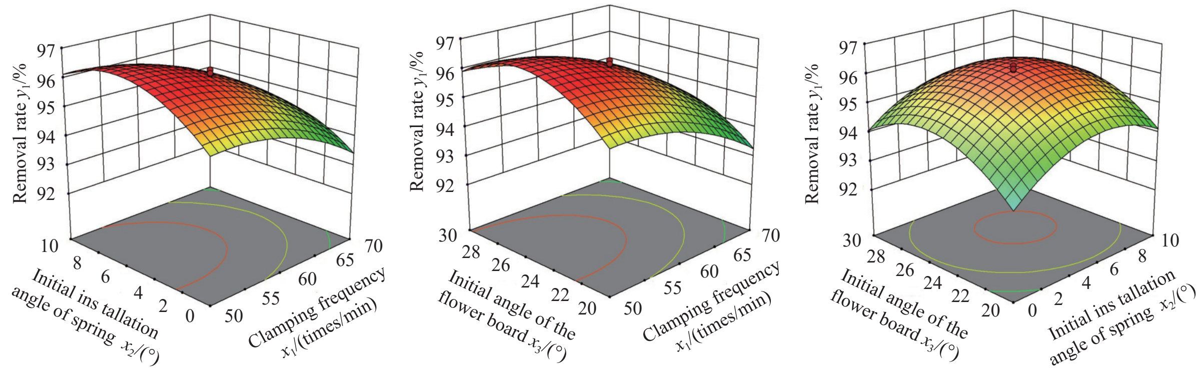

a. $y_1=f(x_1, x_2, 25)$ b. $y_1=f(x_1, 50, x_3)$ c. $y_1=f(60, x_2, x_3)$

Figure 4 Effects of interaction on removal rate

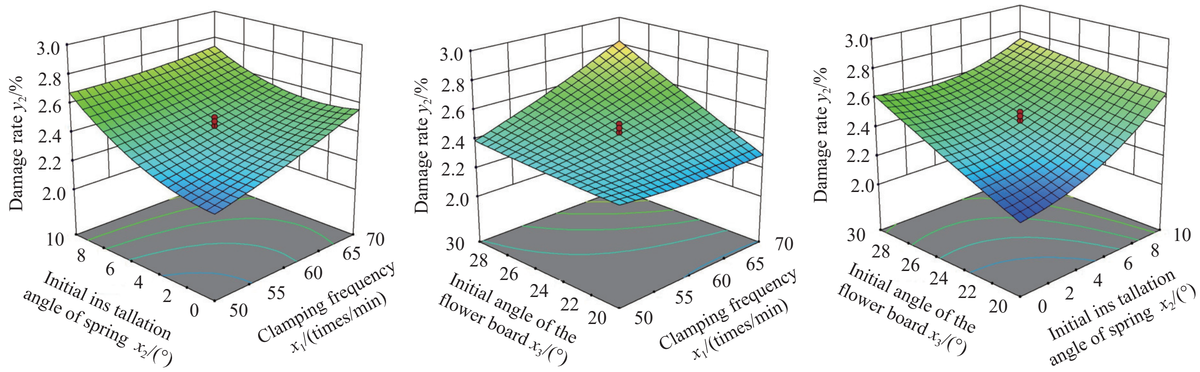

a. $y_2=f(x_1, x_2, 25)$ b. $y_2=f(x_1, 50, x_3)$ c. $y_2=f(60, x_2, x_3)$

Figure 5 Effects of interaction on damage rate

removal rate when the initial installation angle of the spring was 5°. When clamping frequency was fixed, the removal rate of safflower filaments first increased and then decreased as the initial angle of the flower board increased. With flower board angle held constant, filament removal displayed nonlinear ascent followed by asymptotic convergence over decreasing clamping frequencies. The maximum removal rate of safflower filaments occurred at a clamping frequency of 50 times/min and an initial flower board angle of 25°.

Figure 4c is a response surface diagram of the effect of the initial installation angle of the spring and initial angle of the flower board on the removal rate when the clamping frequency was fixed at 60 r/min. With the increase of the initial installation angle of the spring and initial angle of the flower board, the removal rate of safflower filaments first increased and then decreased. The removal rate was the largest when the initial installation angle of the spring was 5° and the initial angle of the flower board was 25°.

Using the maximum removal rate as the evaluation index, an optimal combination of parameters was obtained by regression formula and software: the clamping frequency was 52.49 times/min, the initial installation angle of the spring was 4.72°, and the initial angle of the flower board was 25.58°. Considering the actual working conditions, the optimized parameters were adjusted to values as follows: the clamping frequency was 52.5 times/min, the initial installation angle of the spring was 4.7°, and the initial angle of the flower board was 25.6°.

4.2.2 Analysis of effects of the factors on the damage rate

Figure 5a is a response surface diagram of the effect of the clamping frequency and the initial installation angle of the spring on the damage rate when the initial angle of the flower board was 25°. When the clamping frequency was constant, the damage rate increased with the increase of the initial installation angle of the spring. Under fixed initial installation angle of the spring, the damage rate progressively declined as clamping frequency increased. When the clamping frequency was 50 times/min and the initial installation angle of the spring was 0°, the damage rate reached the minimum value.

Figure 5b is a response surface diagram of the effect of the clamping frequency and initial angle of the flower board on the damage rate when the initial installation angle of the spring was 5°. The damage rate decreased first and then tended to flatten with the decrease of the clamping frequency and initial angle of the flower board. The damage rate was the smallest when the clamping frequency was 50 times/min and initial angle of the flower board was 20°.

Figure 5c is a response surface diagram of the effect of the initial installation angle of the spring and initial angle of the flower board on the damage rate when the clamping frequency was fixed at 60 times/min. When the initial installation angle of the spring was constant, the damage rate decreased with the decrease of the initial angle of the flower board. With the initial angle of the flower board held constant, the damage rate progressively increased as the initial installation angle of the spring increased. Minimum damage rate was observed with the initial flower board angle set at 20° and the spring installation angle at 0°.

Using the minimum damage rate as the evaluation index, an optimal combination of parameters was obtained according to the regression formula and software: the clamping frequency was 51.15 r/min, the initial installation angle of the spring was 0.035°, and the initial angle of the flower board was 20.1°. Accounting for operational constraints, we implemented the following adjusted parameters: 51 r/min clamping frequency, 0° spring installation angle, and 20° flower board angle.

4.3 Parameter optimization

Based on the importance of two indicators, a weighted comprehensive scoring method was used. The weight of the removal rate was 0.5, the weight of the damage rate was 0.5, and the weighted values were used as evaluation criteria. The software Design-Expert 11 was used to optimize the combination of parameters to meet the performance requirements.

Objective function:

$$\max\ y(x_1,x_2,x_3)=0.5y_1+0.5y_2,\begin{cases}\max y\\ 50\le x_1\le 70\\ 0\le x_2\le 10\\ 20\le x_3\le 30\end{cases} \tag{5}$$

The optimal combination of influence parameters was as follows: the clamping frequency was 50 r/min, the initial installation angle of the spring was 3.2°, and the initial angle of the flower board was 24.97°. At this time, the removal rate was 96.28% and the damage rate was 2.29%.

5 Verification

5.1 Camera experimental device

Camera equipment was connected to the side of the experimental device (Figure 6).

Figure 6 Camera experimental device

The camera equipment included cameras (Honor 20 mobile phone, rear 48 megapixels, f/2.2 aperture, supporting 1080P 30 fps slow motion shooting, China) and a computer (Think Pad E580, Lenovo, China) .

The slow lens in mobile phone cameras is properly used so that the movement process of the safflower filaments in the shield can be clearly captured. The flow states of the safflower filaments before and after optimization of experimental parameters were compared and analyzed.

5.2 Image analysis

Derived from optimization, the experimental parameters yielded the following configuration: clamping frequency at 50 times/min, spring installation angle at 3.2°, and initial angle of the flower board at 25°. The image of the high-speed camera experiment is shown in Figure 7.

a. Filaments in process of clamping b. After the filaments clamped

Figure 7 Experimental images of optimization group

The parameters of the comparison group were adjusted to values as follows: the working speed was 52.5 r/min, the initial installation angle of the spring was 4.76°, and the clip angle was 25.6°. Experimental results are shown in Figure 8. These parameters are those of the safflower flexible clamping device when the maximum removal rate is obtained in the test.

a. Filaments in process of clamping b. After the filaments clamped

Figure 8 Experimental images of control group

In the stage in which the safflower filaments were clamped by the clip flower board, by comparing Figure 7a with Figure 8a, it can be seen that in the optimization group, the safflower filaments on the flower buds can be coated by the clip flower board, and the filigree clamping effect is basically the same as in the conditions when the maximum removal rate was obtained in the test, and there were almost no residual filaments on the flower buds after harvesting.

By comparing Figure 7b with Figure 8b, it can be seen that there were less damaged filaments in the harvested filigree, and there were no filaments that were bonded to lumps due to breakage in the optimization group, which would not affect the filigree quality. According to the experimental analysis, the filament harvesting capacity of the flexible clamping device was retained, and the damage to the filigree during the harvesting process was greatly reduced.

In the three experiments of the optimization group, the removal rates were 96.25%, 96.24%, and 96.28%, respectively. The damage rates were 2.29%, 2.3%, and 2.33%, respectively.

Compared with the values of Table 3, the damage rate of the filaments was at a lower value, indicating that there were fewer cracked filaments. In addition, the filigree clamping effect was basically the same as that of the highest removal rate in the previous test, indicating that the harvesting performance of the flexible clamping device is better than before.

6 Discussion

1) The experimental material used in this study was Yumin thornless safflower. Clamping frequency, spring installation angle, and flower board angle were analyzed as influencing factors for device harvesting performance and filament damage resistance. Reduced clamping frequency enhanced operational outcomes: increased removal rate, decreased damage rate, and improved harvesting efficacy. When the initial installation angle of the spring increased, the removal rate increased, but due to the increase in the initial installation angle of the spring, the clamping force applied to the filament increased, resulting in an increase in filament damage rate. When the initial angle of the flower board was greater than 25°, the position of the filament gripping was higher, resulting in a lower removal rate and higher damage rate. When the initial angle of the flower board was less than 25° and gradually decreased, the removal rate gradually decreased and the damage rate decreased.

When the initial angle of the flower board was 20°, the harvesting performance and anti-damage ability were the best.

2) During the harvesting process, the gripping force on the filaments varies under different initial installation angles of the spring, and the gripping position of the filaments also varies at different gripping angles, which is the main reason for the change in the damage rate of the filaments. The harvesting status of the device before and after optimization was verified using photography experiments, and the main reasons for filament damage were analyzed. The harvesting performance and damage resistance of the safflower flexible gripping device were optimized.

7 Conclusions

The flexible clamping device for safflower has been designed, and the design requirements, overall structure, and working principle were illustrated.

1) This research analyzed the factors that influenced the harvesting performance of the flexible clamping device for safflower, explored the mechanism of the clamping effect of the flower board on the filament during the harvesting process, and determined the structure parameters of the system based on the analysis results.

2) The experimental design incorporated three key variables—clamping frequency, spring installation angle, and flower board angle—with removal and damage rates serving as primary performance metrics. Optimal device performance (96.28% removal rate, 2.29% damage rate) was achieved at 50 times/min clamping frequency, 3.2° spring installation, and 25° flower board angle, establishing peak harvesting efficiency with minimal loss. The system designed in this study met the requirements for safflower harvesting.

Acknowledgement

This study was supported by the Natural Science Foundation of Xinjiang Uygur Autonomous Region (Grant No. 2022D01B30).

[References]

[1] Delshad E, Yousefi M, Sasannezhad P, Rakhshandeh H, Ayati Z. Medical uses of *Carthamus tinctorius* L. (Safflower): a comprehensive review from traditional medicine to modern medicine. Electron Physician, 2018; 10(4): 6672–6681.

[2] Yang Y, Huang X L, Jiang Z M, Keshang Aduma, Han Y C, Yu J, et al. New research progress for chemical compositions and pharmacological effect of *carthamus tinctorius* L. Chinese Archives of Traditional Chinese Medicine, 2023; 41(10): 119–126.

[3] Adamska I, Biernacka P. Bioactive substances in safflower flowers and their applicability in medicine and health-promoting foods. Int J Food Sci, 2021; 6657639. doi: 10.1155/2021/6657639.

[4] Liu B B, Dong Y, Yao C, Jiang F Q. Survey on resource development of saffron in China. Chin J Mod App.Pharm, 2022; 39(13): 1783–1788.

[5] Li D Z. Yumin County, Xinjiang: The safflower industry is booming. Farmers Daily, 2022-06-08(003) (in Chinese)

[6] Zhou Y H, Guo J F, Ma X L et al. Research on current situation and development countermeasures of Xinjiang safflower production. Journal of Anhui Agricultural Sciences, 2021; 49(19): 199–201, 217. doi: 10.3969/j. issn.0517-6611.2021.19.052 (in Chinese)

[7] Ge Y, Zhang L X, Han D D, Chen J P, Fu W. Current state and development trend of the mechanical harvesting on saffron filaments. Journal of Agricultural Mechanization Research, 2014; 11: 265–268.

[8] Ge Y, Zhang L X, Gu J W, Fu W, Zhu R G, Zhang H M. Parameter optimization and experiment of dual roller harvesting device for safflower. Transactions of the CSAE, 2015; 31(21): 35–42.

[9] Denarda A R, Bertetto A M, Carbone G. Designing a low-cost mechatronic device for semi-automatic saffron harvesting. Machines, 2021; 9(5): 94. doi: 10.3390/machines9050094

[10] Yang H F. Research status of mechanized harvesting of safflower silk in Xinjiang. Agricultural mechanization in Xinjiang, 2020; 5: 34–37. doi:10.13620/j. cnki.issn1007-7782.2020. 05.009. (in Chinese)

[11] Liu G X, Ge Y, Zhang L X, Zhao Q Z, Zhang T Y. Design of cutting safflower picking experiment platform and experimental study on picking performance. Machine Design and Research, 2019; 35(2): 178–183.

[12] Jiao X P, Ge Y, Zhang L X, Liang D D, Liu G X, Zhang T Y. The design of the key components of the cutting device of cutting type safflower harvester. Machine design and research, 2017; 33(3): 161–164.

[13] Zhang Z G, Zhao M, Xing Z Y, Liu X F. Design and test of double-acting opposite direction cutting end effector for safflower harvester. Transactions of the CSAM, 2022; 53(12): 160–170.

[14] Zhang Z G, Lv Q G, Ren J Y, Han C J, Yuan P P, Zhang X J. Design of critical components for safflower harvesting machinery by rotary shear. Journal of Chinese Agricultural Mechanization, 2019; 40(7): 1–6.

[15] Zhang X W, Ge Y, Chen F, Yu P F. Design of three-finger pull-out safflower picking end effector. Mechanical Design and Manufacturing, 2022; 1: 145–149.

[16] Cao W B, Yang S P, Li S F, Jiao H B, Lian G D, Niu C, An L L. Parameter optimization of height limiting device for comb-type safflower harvesting machine. Transactions of the CSAE, 2019; 35(14): 48–56.

[17] Cao W B, Lian G D, Niu C, An L L, Yang S P, Chen B B. Harvest performance test and parameter optimization of comb-type safflower-filaments picking head at same height. Transactions of the CSAE, 2018; 34(22): 36–44.

[18] Zhang T Y, Zhang L X, Ge Y, Liu G X, Zhang X W. Development and test of a portable roller-type safflower harvester. Agricultural mechanization research, 2020; 42(3): 76–81.

[19] Chen F, Ge Y, Zhang L X, Zhang X W, Xia Y Q. Simulation and optimization design and experiment of airflow field in safflower picking chamber. Journal of Jiangsu University (Natural Science Edition), 2021; 42(4): 414–420.

[20] Hu Z Z. Design and research of pneumatic safflower cleaning device. Shihezi University, 2023. doi: 10.27332/d.cnki.gshzu.2022.000127. (in Chinese)

[21] Wu D L, Yuan J H, Li C, Jiang S, Ding D, Cao C M. Design and experiment of twist-comb end effector for picking camellia fruit. Transactions of the CSAM, 2021; 52(4): 21–33.

[22] Ma S J. Improvement design and experimental research on key components of tobacco leaf picking mechanism. Henan Agricultural University, 2022. doi: 10.27117/d.cnki.ghenu.2022.000447. (in Chinese)

[23] Huang J C, Zhang B, Tian K P, Liu H L, Shen C. Design and optimization of the parameters of the key components for reed harvester. Int J Agric & Biol Eng, 2022; 15(6): 96–103.

[24] Yuan J B, Wang J F, Li H, Qi X D, Wang Y J, Li C. Optimization of the cylindrical sieves for separating threshed rice mixture using EDEM. Int J Agric & Biol Eng, 2022; 15(2): 236–247.

[25] Chen M Z, Xu G F, Wei M J, Li X W, Wei Y Z, Diao P S, et al. Optimization design and experiment on feeding and chopping device of silage maize harvester. Int J Agric & Biol Eng, 2023; 16(3): 64–77.

[26] Zhang Z G, Zeng C, Xu P, Shi R M, Wang Y Z, Xing Z Y. Clamping root-cutting end-effector for harvesting fresh safflower. Int J Agric & Biol Eng, 2025; 18(2): 146–154.

[27] Zhang Z G, Zeng C, Xing Z Y, Xu P, Guo Q F, Shi R M, et al. Discrete element modeling and parameter calibration of safflower biomechanical properties. Int J Agric & Biol Eng, 2024; 17(2): 37–46.